Entropic Spring with Monte Carlo

Feix Filson

October 26, 2025

1 Introduction

The goal of this project was to reproduce Hooke's law for an idealised entropic spring using Monte Carlo (MC) methods. A 1D rubber band of N links, each of length a, was simulated. Each link could point in either the + or − direction. The total length of the rubber band was then given by

$$L = a(2n - N), \tag{1}$$

where n is the number of + links. By counting microstates for a given L, the entropy is approximately given by

$$S \approx k_B N \ln 2 - \frac{k_B L^2}{2Na^2}. \tag{2}$$

This leads to an entropic force given by

$$f = -T\frac{\partial S}{\partial L} = \frac{k_B T}{Na^2}L. \tag{3}$$

The chain, therefore, behaves as an ideal spring with an effective spring constant $k_{\text{eff}} = k_B T/(Na^2)$. The simulation aims to verify this relationship numerically and to study the breakdown of the linear regime.

2 Method

2.1 Unbiased Simulation (Task I)

The purpose of the first task was to simulate a rubber band with an unbiased distribution of + and − distributions, I.E. both directions are equally likely. Each configuration of N links was generated randomly with equal probability for + and −. The total extension L was computed for each configuration using equation 1 and then plotted in a histogram to estimate $P(L)$. An analytic reference distribution was then plotted on top for comparison, given by

$$P(L) = \frac{1}{2^N}\Omega(N, n), \tag{4}$$

where

$$\Omega(N, n) = \binom{N}{n}, \tag{5}$$

and

$$n = \frac{L/a + N}{2}, \tag{6}$$

where equation 6 is a rewritten version of 1.

Further comparisons were made using a ratio plot and a χ^2/ndf statistic to quantify the agreement.

2.2 Reweighting (Task II)

The purpose of the second task was to simulate a rubber band when an external force f is applied without resampling. This was done by reweighting the unbiased configurations using

$$w_i = e^{\beta f L_i}, \tag{7}$$

where $\beta = \frac{1}{k_B T}$. The weighted configurations were plotted in a histogram and compared to the analytic distribution curve given by

$$P_f(L) = \frac{\Omega(N,n)e^{\beta f L}}{Z(f)}, \tag{8}$$

where

$$Z(f) = \sum_L \Omega(N,n)e^{\beta f L}. \tag{9}$$

This was done in the small force range ($f \in [0.01, 0, 1]$ and for a larger force range ($f \in [0.1, 1.0]$. For the larger force range, the reweighting was diagnosed by calculating the effective number of samples using

$$\mu_{\text{eff}} = \frac{1}{\sum_i \tilde{w}_i^2}, \tag{10}$$

where $\quad \tilde{w}_i = \frac{w_i}{\sum_j w_j}$.

2.3 Direct Biased Simulation (Task III)

For large f reweighting was not a suitable method. To simulate these situations accurately, the links are re-sampled with a bias towards the + direction. The probability of a link pointing in the + direction was calculated using

$$p_+(f) = \frac{e^{\beta f a}}{e^{\beta f a} + e^{-\beta f a}} = \frac{1}{2}\big[1 + \tanh(\beta f a)\big]. \tag{11}$$

Given this probability, the mean extension was given by

$$\langle L \rangle(f) = Na\tanh(\beta f a), \tag{12}$$

which, in the small force limit, reduces to

$$\langle L \rangle \approx \frac{Na^2}{k_B T} f. \tag{13}$$

This is the same form as Hooke's law, with the spring constant $k = k_B T/(Na^2)$. Both these $\langle L \rangle$ were plotted with and compared to the average length of the sampled bands for each force. An estimate of the spring constant k_{eff} was calculated by fitting the MC data.

3 Results

3.1 Task I: Unbiased Distribution

Figure 1 shows the distribution of the ratio L/a using unbiased MC sampling of 10^6 bands and the analytic reference (equation (4)). The ratio plot and χ^2/ndf value indicate good agreement between the two datasets.

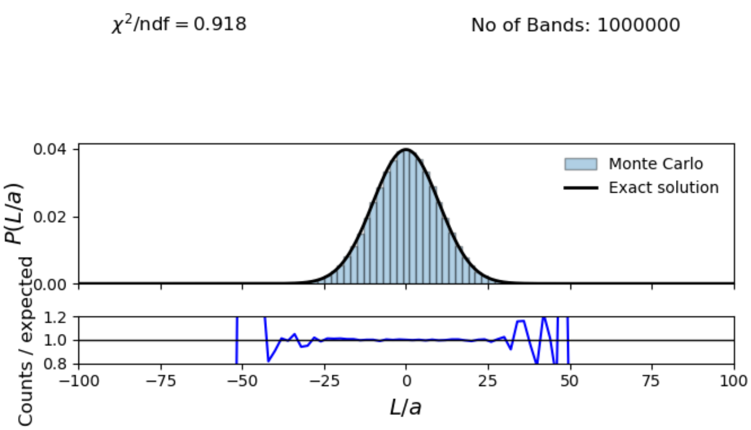

Figure 1: Unbiased distribution $P(L)$ for $N = 100, a = 1$. The histogram shows MC results with an analytic binomial distribution curve on top. The ratio panel (bottom) and χ^2/ndf quantify agreement.

3.2 Task II: Reweighting under Force

Figure 2 shows the new distributions when a small force is applied. The histograms were created by reweighting the unbiased distribution using the weights from equation (7). The analytic curves on top were given by equation (8). In this force range, the reweighting gave accurate results, as can be seen in the ratio plots. Figure 3 shows the same plots for larger forces. Very clearly, the reweighting here breaks down. The plot of μ_{eff} in figure 4 shows the reason for this; the effective sample size collapses as a function of f.

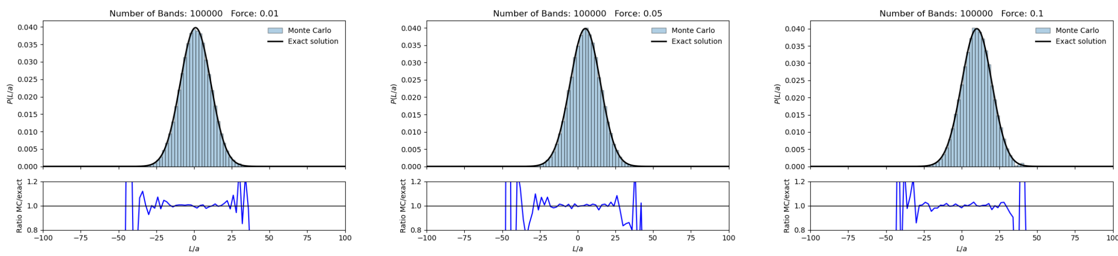

(a) $f = 0.01$ (b) $f = 0.05$ (c) $f = 0.10$

Figure 2: Weighted distributions $P_f(L)$ in the small-force regime. Reweighting agrees with the analytic prediction and ratio panels remain flat within uncertainties.

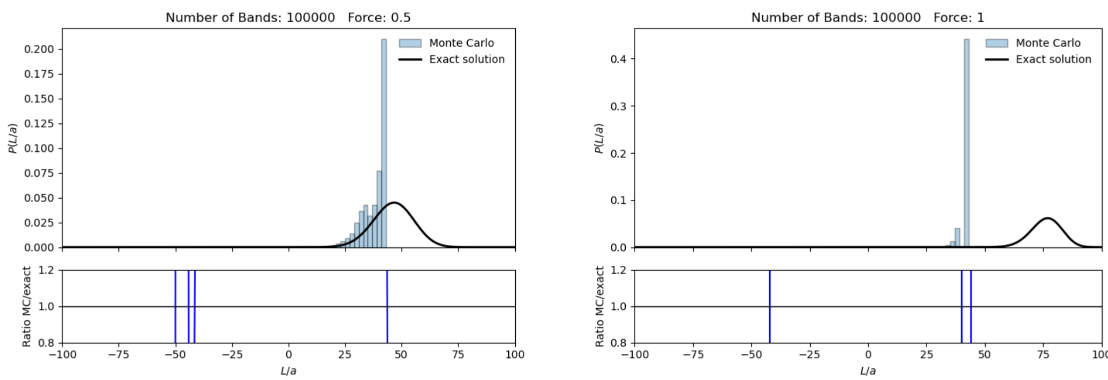

(a) $f = 0.50$ (b) $f = 1.00$

Figure 3: High-force regime where reweighting breaks down. Deviations from the analytic curve and non-flat ratios appear as ensemble overlap vanishes (effective sample size drops).

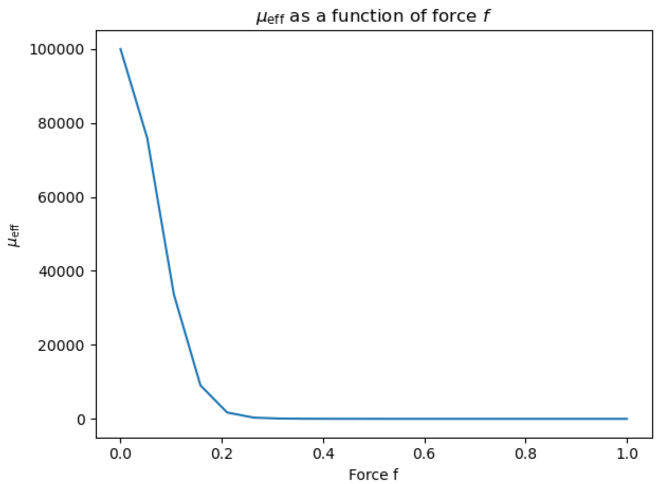

Figure 4: Effective sample size μ_{eff} versus f. Reweighting becomes unreliable once $\mu_{\mathrm{eff}}/M \lesssim 0.1$.

3.3 Task III: Direct Biased Sampling

Figure 5 shows the average length as a function of the force f using biassed sampling (equation 11), the analytic average given the bias (equation 12), and the Hookean average (equation 13). Table 1 presents the spring constant after fitting the MC data and compares it to the prediction from equation 13, which show good agreement. Figure 6 shows that the standard deviation of the length L as a function of the force decreases as the force increases. Figure 7 shows that in the large force range, the distribution shifts and narrows. Figure 8 shows how the analytic curve and the MC strongly diverge from Hooke's law.

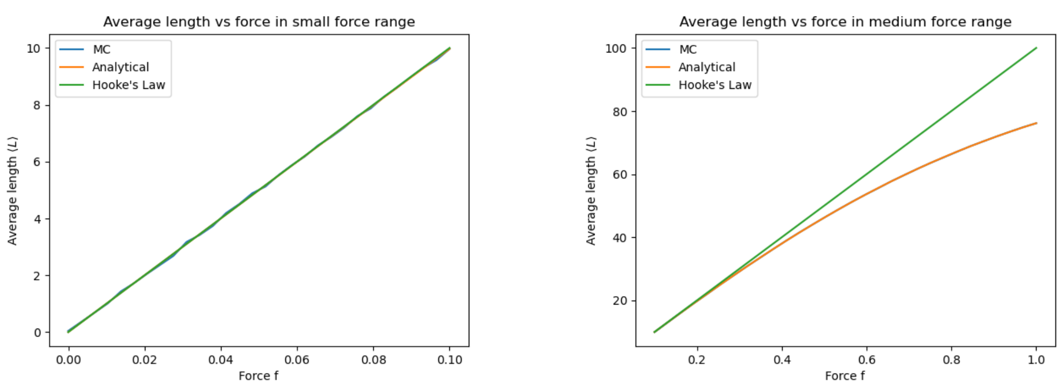

(a) Small-f range

(b) Medium-f range

Figure 5: Mean extension $\langle L\rangle(f)$ compared to the analytic prediction $Na\tanh(\beta fa)$. The dashed line shows the linear (Hookean) approximation. Left: small-f region with excellent agreement to the linear model. Right: medium-f region where deviations from linearity begin.

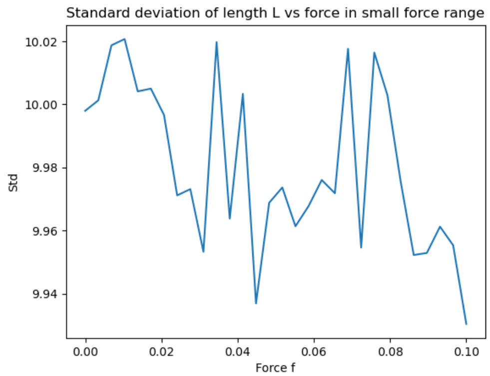

(a) Small-f range

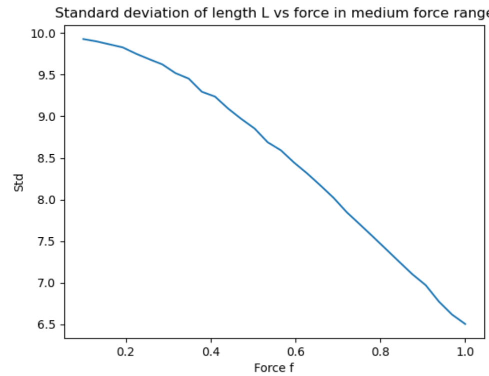

(b) Medium-f range

Figure 6: Standard deviation $\sigma_L(f)$ of the extension versus force. The analytic reference can be overlaid as a solid curve (e.g., from the binomial/tanh model). Left: small-f fluctuations near the linear regime. Right: medium-f behaviour as the distribution narrows and nonlinearity grows.

Parameter	Value	Analytic Expectation
N	100	–
a	1	–
k_{eff}	0.009946	$k_BT/(Na^2) = 0.0100$

Table 1: Extracted spring constant from the linear fit compared to analytic expectation (for $k_BT = 1$).

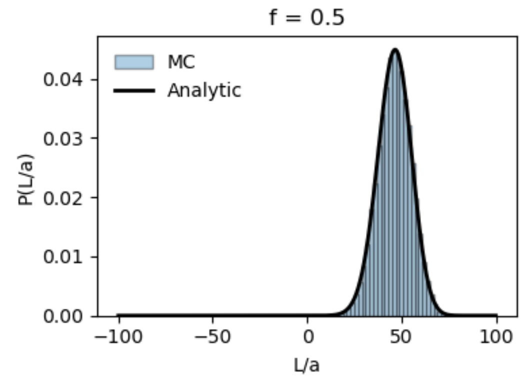

(a) $f = 0.5$

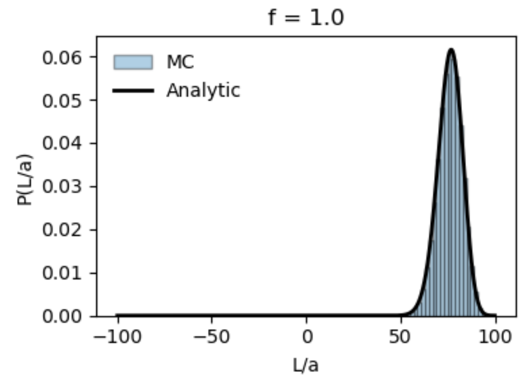

(b) $f = 1$

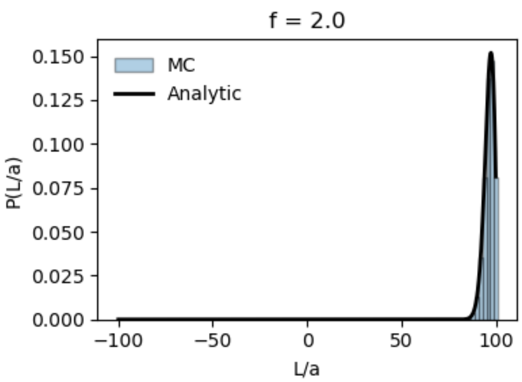

(c) $f = 2$

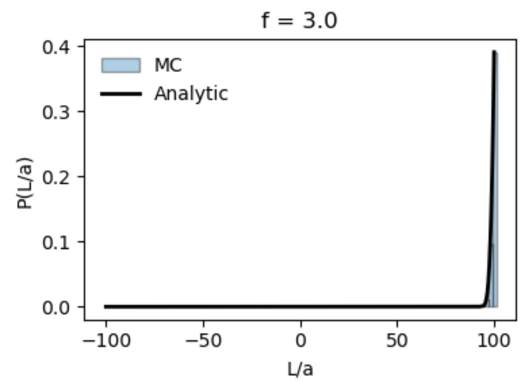

(d) $f = 3$

Figure 7: Biased distributions $P_f(L)$ at large f. The peak shifts strongly toward large L and the distribution becomes narrow (small σ_L), indicating strong bias and loss of ensemble overlap with the unbiased sample.

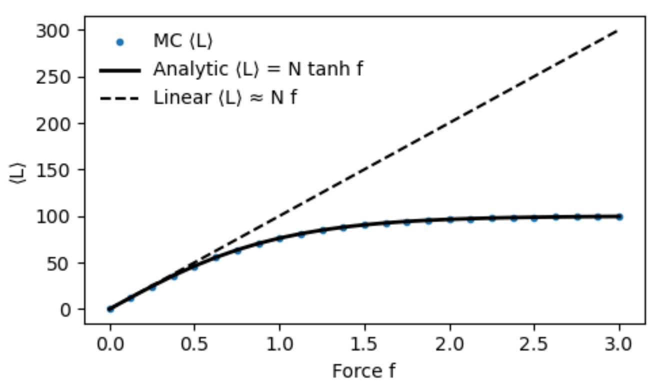

Figure 8: Breakdown of Hooke's law at large f. The Monte Carlo data for the mean extension $\langle L\rangle(f)$ (points) follow the full analytic prediction $Na\tanh(\beta fa)$ (solid curve) and deviate strongly from the linear (Hookean) approximation $Na^2\beta f$ (dashed line), demonstrating saturation and nonlinearity of the entropic spring.

4 Discussion

The unbiased simulation reproduced the theoretical distribution $P(L)$ with great precision. The ratio plots were flat around unity and the calculated $\chi^2/\mathrm{ndf} \approx 1$, confirming that the Monte Carlo sampling was statistically consistent with the analytic binomial form.

In the reweighting task, the method performed well for small applied forces ($f \lesssim 0.1$), where the ensemble overlap between the unbiased and biased configurations was still sufficient. The weighted histograms matched the analytic distributions and the ratio panels remained stable. However, as f increased, the reweighting clearly broke down. The reason for this failure is clear from the effective sample size μ_{eff}, which drops sharply with f. At large forces, only a small subset of the unbiased configurations contribute significant weight. This effect causes poor statistics and unreliable distributions. This behaviour directly illustrated the limitations of reweighting when the biased distribution becomes too different from the original one.

The direct biased simulation resolved this issue. By explicitly sampling each link with a bias $p_+(f)$, the simulation produced distributions that remained consistent with the analytic expression for all f. The measured mean extensions $\langle L\rangle(f)$ followed the theoretical $Na\tanh(\beta fa)$ curve very well across the entire force range. In the small-force limit, the results were linear and the fitted spring constant k_{eff} agreed with the predicted value $k_BT/(Na^2)$ well. At intermediate forces, deviations from the linear approximation became visible, and for large f, the system approached saturation where nearly all links were aligned with the field. This non-linear behaviour marked the breakdown of Hooke's law. The trends in the mean and standard deviation of L with f matched the expected narrowing of the distribution as entropy is reduced under strong alignment.

5 Conclusions

This project confirmed through Monte Carlo simulation that a one-dimensional chain of binary links behaves as an entropic spring. The simulations reproduced Hooke's law in the low-force regime and quantitatively matched the theoretical spring constant $k_{\mathrm{eff}} = k_BT/(Na^2)$. The reweighting study demonstrated the range of validity of small-bias corrections and provided a clear numerical example of how statistical overlap limits this approach. By switching to direct biased sampling, the full non-linear force–extension relationship $\langle L\rangle = Na\tanh(\beta fa)$ was recovered, and the transition from linear to saturated behaviour was clearly observed.

In summary, the Monte Carlo results agree with analytic predictions across all regimes. The spring constant extracted from the simulation matched theory to within the statistical error, and the breakdown of the linear approximation at large f was clearly visible. The project successfully linked microscopic statistical behaviour to macroscopic elastic properties, illustrating how Hooke's law emerges—and eventually fails.